

Article

Quasar Black Hole Mass Estimates from High-Ionization Lines: Breaking a Taboo?

Paola Marziani ^{1,*} , Ascensión del Olmo ^{2,*}, Mary Loli Martínez-Aldama ², Deborah Dultzin ³, Alenka Negrete ³, Edi Bon ⁴, Natasa Bon ⁴ and Mauro D'Onofrio ⁵

¹ Osservatorio Astronomico di Padova, Istituto Nazionale di Astrofisica (INAF), IT 35122 Padova, Italy

² Instituto de Astrofísica de Andalucía (IAA-CSIC), E-18008 Granada, Spain; maryloli@iaa.es

³ Instituto de Astronomía, Universidad Nacional Autónoma de México (UNAM), México D.F. 04510, Mexico; deborah@astro.unam.mx (D.D.); alenka@astro.unam.mx (A.N.)

⁴ Astronomical Observatory, Volgina 7, 11060 Belgrade 38, Serbia; ebon@oab.rs (E.B.); nbon@oab.rs (N.B.)

⁵ Dipartimento di Fisica & Astronomia “Galileo Galilei”, Università di Padova, IT35122 Padova, Italy; mauro.donofrio@unipd.it

* Correspondence: paola.marziani@oapd.inaf.it (P.M.); chony@iaa.es (A.d.O.)

Academic Editor: Robert C. Forrey

Received: 31 August 2017; Accepted: 14 September 2017; Published: 20 September 2017

Abstract: Can high ionization lines such as CIV λ 1549 provide useful virial broadening estimators for computing the mass of the supermassive black holes that power the quasar phenomenon? The question has been dismissed by several workers as a rhetorical one because blue-shifted, non-virial emission associated with gas outflows is often prominent in CIV λ 1549 line profiles. In this contribution, we first summarize the evidence suggesting that the FWHM of low-ionization lines like H β and MgII λ 2800 provide reliable virial broadening estimators over a broad range of luminosity. We confirm that the line widths of CIV λ 1549 is not immediately offering a virial broadening estimator equivalent to the width of low-ionization lines. However, capitalizing on the results of Coatman et al. (2016) and Sulentic et al. (2017), we suggest a correction to FWHM CIV λ 1549 for Eddington ratio and luminosity effects that, however, remains cumbersome to apply in practice. Intermediate ionization lines (IP \sim 20–30 eV; AlIII λ 1860 and SiIII λ 1892) may provide a better virial broadening estimator for high redshift quasars, but larger samples are needed to assess their reliability. Ultimately, they may be associated with the broad-line region radius estimated from the photoionization method introduced by Negrete et al. (2013) to obtain black hole mass estimates independent from scaling laws.

Keywords: ionization processes; emission line formation; atomic spectroscopy; supermassive black holes; emission line profiles; quasars

1. Introduction: Statement of the Problem

A defining property of type-1 quasars is the presence of broad and narrow optical and UV lines emitted by ionic species over a wide range of ionization potentials (IPs, [1]): high-ionization lines (HILs) involving IP > 50 eV, and low-ionization lines (LILs) from ionic species with IP < 20 eV. Over the years, it has turned expedient to consider the UV resonance line CIV λ 1549 as a representative of broad HILs. Lines do not all show the same profiles, and redshifts measured on different lines often show significant differences. Internal line shifts involving both broad lines in the optical and UV spectra of quasars have offered a powerful diagnostic tool of the quasar innermost structure since a few years after the discovery of quasars [2].

The CIV λ 1549 is a resonant doublet ($^2P_{3/2,1}^o \rightarrow ^2S_{1/2}$) emitted by gas which is, at least in part, flowing out from a region within \sim 1000 gravitational radii from the central black hole (e.g., [3], for a review).

The occurrence of CIV λ 1549 large shifts constrains the suitability of the CIV λ 1549 profile broadening as a virial black hole mass (M_{BH}) estimator (see, e.g., [4,5], for reviews). Results at low-redshift obtained in the mid-2010s suggest that the CIV λ 1549 line is unsuitable for, at least, part of the quasar Population A sources (Section 4 [6]). A similar conclusion was reached at $z \approx 2$ on a sample of 15 high-luminosity quasars [7]. More recent work tends to confirm that the CIV λ 1549 line width is not straightforwardly related to virial broadening (e.g., [8]). However, the CIV λ 1549 line is strong and observable up to $z \approx 6$ with optical spectrometers. It is so highly desirable to have a consistent virial broadening estimate up to the highest redshifts that various attempts (e.g., [9]) have been done at “rehabilitating” CIV λ 1549 line width estimators to bring them in agreement with the width of LILs such as H β and MgII λ 2800 [10].

In this contribution, we briefly stress the importance of black hole mass estimates (Section 2) and recapitulate the basic method of M_{BH} estimates applied to large samples of quasars under the virial assumption (Section 3). To improve estimates that have been known to be plagued by systematic and statistical uncertainties as large as a factor ~ 100 , we adopt the “rehabilitating” power of the quasar eigenvector 1 (E1; Section 4). Our analysis is then focused on virial broadening estimators (VBEs; Section 5) from: (a) LILs (IP < 15 eV: H β , MgII 2800); (b) HILs (IP > 40 eV: CIV λ 1549); (c) intermediate-ionization lines (IILs: SiIII λ 1892, Al III λ 1860), for which we provide a brief summary of preliminary results. Reported results from our group were published during the last decade [11–14]. We finally suggest that “photoionization” computations of M_{BH} (Section 6) may offer a solution to some of the problems associated with the use of an average scaling law.

2. Importance of Black Hole Mass Determination

The relevance of supermassive black hole M_{BH} estimates is not limited to the sake of a better understanding of quasars interpreted as accreting system. Black hole masses are a key parameter in the evolution of the galaxies and in cosmology as well. Massive, fast outflows are affected by the ratio of radiation to gravitational forces. They provide feedback effects to the host galaxy, and are even invoked to account for the M_{BH} -bulge velocity dispersion correlation [15–17]. The ratio between radiation and gravitation forces also influences broad-line region dynamics; lower column density material may flow out of the emitting region [14,18,19]. Black hole masses of high redshift quasars provide constraints on primordial black hole collapse (and references therein [20,21]). Overestimates by a factor as large as ~ 100 for supermassive black holes at high z may even pose a spurious challenge to concordance cosmology. Present-day estimates constrain the relation between the formation of the seed black holes and the collapse of the protogalaxy. Collapse of dark matter clumps yielding massive seeds that then rapidly grows by super-Eddington accretion appears necessary to explain the occurrence of supermassive black holes at very high redshifts.

3. Virial Black Hole Mass Estimates

The virial expression for the mass can be written as

$$M_{\text{BH}} = fr_{\text{BLR}}\delta v^2/G, \quad (1)$$

where f is a factor of order unity reflecting geometry and dynamics of the broad line emitting regions, and r_{BLR} is a representative distance of the broad-line emitting region (BLR).¹ The virial broadening δv is provided by a measurement of the line profile width, which can be velocity dispersion σ , FWHM, or FWZI. The FWHM is by far the most handy measure employed as a VBE although some authors claim that a better estimator may be offered by the velocity dispersion [22]. The latter measure is, however, not defined in the case of Lorentzian profiles and not of easy interpretation in the case of

¹ The following analysis pertains only type 1 quasars showing broad (FWHM > 1000 km s⁻¹) emission in permitted lines.

shifted profiles. The virial assumption had a spectacular confirmation (albeit limited to few cases) by type-1 sources for which several lines were monitored: the response time of the BLR line and the line width were found to be correlated exactly as expected for Keplerian motion around a massive central object, with $\delta v \propto r^{-\frac{1}{2}}$ [23].

We can subdivide the estimates of the radius of the BLR (r_{BLR}) as primary and secondary. Primary determinations are obtained as the peak or centroid of the cross-correlation function between continuum and line light curves. Secondary determinations stem from the correlation between r_{BLR} and luminosity that has been derived from reverberation-mapped sources (e.g., [24–27]): $r_{\text{BLR}} \propto L^a$, $a \approx 0.5–0.65$ [24,28]. The relation takes different form for different lines, and has been defined for H β and CIV. It then becomes possible to derive scaling laws for the black hole mass: $M_{\text{BH}} = M_{\text{BH}}(L, \text{FWHM}) = kL^a \text{FWHM}^b$. If $a = 0.5$, $b = 2$, the relation is consistent with the virial assumption (e.g., [29,30]), and the r_{BLR} scaling laws. If $a \neq 0.5$, $b \neq 2$ (e.g., [31–33]), the mass scaling law still provides M_{BH} estimates, but the accuracy of these estimates is likely to be sample-dependent (see Section 5.3).

The M_{BH} scaling laws provide a simple recipe usable with single-epoch spectra of large sample of quasars. Estimates of the Eddington ratio are derived by applying a bolometric correction to the observed luminosity. The correction is typically assumed a factor 10–13 from the flux λf_{λ} at 5100 Å (measured in erg s^{-1}) and 3.4–5 from λf_{λ} measured at 1450 Å in the UV, [34,35]). For the sake of the present review, we will stay with these constant corrections without forgetting that different bolometric corrections should be defined along the quasar “main sequence” (introduced in Section 4), and that the correction is most likely luminosity as well as orientation dependent [36].

Caveats

The estimate of the M_{BH} is based on several assumptions underlying reverberation mapping studies: among them, a compact region wetting the quasar continuum, and a fairly monotonic response of the line emitting gas. This latter assumption has been apparently challenged by the unpredicted behavior of NGC 5548 in 2014, where a time delay τ much shorter than expected was found when the source was in a high-luminosity state [37–39]. The physical origin of this behavior is not yet clear: in principle, shielding, optically thin gas, changing size of the continuum source could also give rise to a shorter (or a lack of) response to continuum change in the emitting line regions. In addition, periodic signals (in photometric and spectroscopic measurements) have been detected in a number of sources [40], including NGC 5548 (e.g., [41–45]). The origin of the periodicity is as yet unclear as well. A second, supermassive binary black hole has been suggested in some cases [41,46] but, in principle, black holes of masses much smaller than the primary could produce periodic photometric properties without leaving a detectable trace of their gravitational pull on the line profiles. As a matter of fact, the $r_{\text{BLR}}-L$ scaling relation has a non-negligible intrinsic dispersion, which may be, at least in part, accounted for by a dependence of r_{BLR} estimates on the dimensionless accretion rate found in recent work [27].

The basic assumption underlying the search of virial broadening estimators is that a line (or line component) is symmetric and unshifted with respect to the quasar rest frame. Most line profiles are asymmetric, and shifted, but this has been ignored until recent years. If CIV FWHM is employed as a virial broadening estimator, the loss of information is so severe that the M_{BH} distribution as a function of redshift cannot be distinguished if masses obtained from random values of the FWHM (e.g., [47]) are used in place of the actual estimates.

A single value of the structure factor is obtained by scaling the M_{BH} to agree with the dynamical masses [48–52]. We expect that the geometry and dynamics of the BLR is related to the accretion mode, although it is as yet not unclear in which way. The structure factor is therefore likely to be different for different type-1 quasar populations. For Populations A and B (defined in Section 4), Collin et al. [53] find $f(\text{FWHM}) \approx 2$ and 0.5, respectively.

4. The Rehabilitating Power of Eigenvector 1

The eigenvector 1 (E1) was originally defined by a principal component analysis of ≈ 80 Palomar–Green quasars, and is associated with an anti-correlation between the strength of the FeII λ 4570 blend, measured by the flux ratio $R_{\text{FeII}} = F(\text{FeII}\lambda 4570)/F(\text{H}\beta)$ and the FWHM of H β . The E1 is (at the very least) an useful tool to organize quasar diversity through a sequence (the main sequence, MS) in the so-called optical plane of the E1, defined by FWHM(H β) vs. R_{FeII} . The 4D E1 parameters space includes two more parameters: the soft X-ray photon index Γ_{soft} associated with the accretion status, and the centroid at half maximum of CIV λ 1549 c(1/2) CIV measuring the amplitude of the high ionization outflow originating from the BLR [54]. More parameters, however, correlate with E1 (see Table 1 of Sulentic et al. [55] and Fraix-Burnet et al. [56]). Since the analysis of Boroson and Green [57], MS trends have been found in works dealing with a number of phenomenological and physical correlates [58–65]. Recently, large Sloan Digital Sky Survey (SDSS) data samples were involved [9,66–69]. The E1 “rehabilitating” power stems, in this context, by the ability to identify systematic trends that may be missed and confused as statistical errors if structurally different sources are dumped together in a single sample.

The trends along the MS allow for the definition of spectral types [70] in bins of $\Delta R_{\text{FeII}} = 0.5$ (A1, A2, A3, A4 from $R_{\text{FeII}} = 0$ to $R_{\text{FeII}} = 2$, tracing a change of L/L_{Edd} convolved with orientation, [71]) and FWHM (A for FWHM H $\beta < 4000 \text{ km s}^{-1}$, B1, B1⁺, B1⁺⁺ for broader sources in steps of 4000 km s^{-1} , tracing mainly a change in orientation). Quasars can be classified as belonging to two quasar Populations, A and B [72]. Population A (FWHM H $\beta < 4000 \text{ km/s}$) includes NLSy1s. Population A and B(roader) sources are most likely associated with a different accretion mode, since Population A are at $L/L_{\text{Edd}} > 0.2\text{--}0.3$ which is the theoretical limit above and is an optically and geometrically thick advection-dominated accretion disk forms [73]. Population B of low L/L_{Edd} may be consistent with a flat α disk. The distinction between Populations A and B separates sources that are also called wind- and disk-dominated by Richards et al. [66], or Populations 1 and 2 by Collin et al. [53]. It supersedes the distinction between NLSy1s and rest of type-1 AGNs, which is based on a FWHM limit that has played an important historical role but is physically arbitrary. At low $z (< 0.7)$, Population A show low M_{BH} , high L/L_{Edd} Population B, high M_{BH} , low L/L_{Edd} , a reflection of the “downsizing” of nuclear activity: practically no black hole with very large mass ($M_{\text{BH}} \sim 10^9\text{--}10^{10} M_{\odot}$) is accreting super-Eddington in the local Universe.

5. Virial Broadening Estimators along the Quasar MS

5.1. LILs: H β and MgII λ 2800

The profiles of LILs like H β and MgII λ 2800 change along the quasar MS. If we want to extract a VBE, we have to consider the behavior of H β and MgII λ 2800 from extreme Population B to extreme Population A.

In Population B, the broad profiles of H β and MgII λ 2800 are most frequently redward asymmetric. Composite spectra of individual spectral types can be modeled by a broad Gaussian component (the BC, symmetric and unshifted, assumed to be the virialized component), and a redshifted very-broad Gaussian component. This latter component presumably associated with “perturbed” virialized motions or gravitational redshift in the inner BLR [74] systematically increases the line width with respect to the BC that provides the VBE.

At the other end of the MS extreme, Population A sources show narrower, Lorentzian-like profiles, slightly blueward asymmetric. The H β and MgII profiles can be modeled by Lorentzian functions plus a blueshifted excess modeled with a skewed Gaussian [12,13]. Both the LIL resonance line MgII λ 2800 and H β are affected by low-ionization outflows detected in the extreme Population A corresponding to spectral types A3–A4 [13]. However, in most of Population A, the LILs are dominated by a symmetric, virialized broad component [8,13,30,75].

We can define a parameter ζ yielding a correction to the observed profile to obtain a VBE, as follows:

$$\zeta = \frac{FWHM_{VBE}}{FWHM_{obs}} \approx \frac{FWHM_{BC}}{FWHM_{obs}} \approx \frac{FWHM_{symm}}{FWHM_{obs}}, \quad (2)$$

where the VBE FWHM can be considered best estimated by the FWHM of the broad component $FWHM_{BC}$, whose proxy can be obtained by symmetrizing the observed FWHM by various corrections described below. Even if the non-virial broadening mechanism is different along the E1 sequence, $0.75 \leq \zeta \leq 1.0$ for both $H\beta$ and $MgII$. This implies that, even if LILs are not always asymmetric, a modest correction is, on average, sufficient to retrieve a VBE from the observed FWHM. Table 1 reports the current estimates along with bibliographic references.

Table 1. The LIL and IIL ζ (Equation 2) factor for the spectral types of the quasar MS, listed for the spectral types (SpT) of highest occupation.

SpT	H β	MgII	AIII	Ref.
A3–A4	0.8/0.9	0.75/0.8	1.0	[12,76]
A1–A2	1.0	1.0	1.0	[12,76]
B1	0.8	0.9	1.35	[13,45]
B1+/B1++	0.8	0.9	1.35	[13,45]

5.2. LIL VBE at High L

At low z , the quasar population reaches bolometric luminosity $\sim 10^{47}$ erg s^{-1} at most. It is interesting to consider the LIL VBE behavior if we add to a local sample sources more luminous than this limit. Composite spectra are helpful to outline the LIL $H\beta$ behavior over a wide luminosity range. Marziani et al. [11] computed composites in step of 1 dex for 6 dex in luminosity, joining an HE/ISAAC high- L sample (52 sources) and an SDSS sample from Zamfir et al. [77]. The $H\beta$ line becomes broader with increasing L (over $43 < \log L < 48.5$ [erg/s]), but shapes are similar: the Population A/Population B differences are preserved at high L [11]. At the same time, the minimum $FWHM(H\beta)$ increases with luminosity. This result is consistent with the virial assumption and with the r_{BLR} scaling law:

$$M_{BH} \propto r_{BLR} FWHM^2 \propto L^a FWHM^2 \propto (L/M)^{-1} L^{(1-2a)/2}. \quad (3)$$

The minimum, luminosity-dependent FWHM is obtained for a limiting Eddington ratio ≈ 1 . As a consequence, the Population A limit is also luminosity dependent.

Extracting a VBE from LIL $H\beta$ at high- L is possible by employing different symmetrization methods:

- substitution of the BC in place of the full $H\beta$ profile. This method requires a multicomponent maximum likelihood fitting, and is fairly reliable for Population A (even for extreme Population A) and Population B spectral types where the VBC is creating a profile inflection;
- symmetrization of the profile: $FWHM_{symm} = FWHM - 2 c(1/2)$;
- correction based on spectral type. In practice, this means to correct $H\beta$ for Population B sources by a factor ζ as reported in Table 1.

All symmetrization methods were found to be equivalent at low- and high- L [45]. In other words, the $H\beta$ profile shapes at high L are consistent with those at low- z , lower L (with some caveats, [11]).

5.3. CIV

Virial broadening estimators extracted from the HIL $CIV\lambda 1549$ along the E1 sequence are unfortunately not easy to define. If we scale the $H\beta$ emission and overlay it on $CIV\lambda 1549$ (Figure 1), we obtain a strong excess of blueshifted emission. The profile can be interpreted as an almost symmetric,

unshifted “virialized” emitting region + an outflow/wind component that dominates in A3/A4 spectral types (e.g., [78–81]) and at high luminosity. The largest shifts of CIV λ 1549 centroid at 1/2 along the MS are found in Population A [4,6,14].

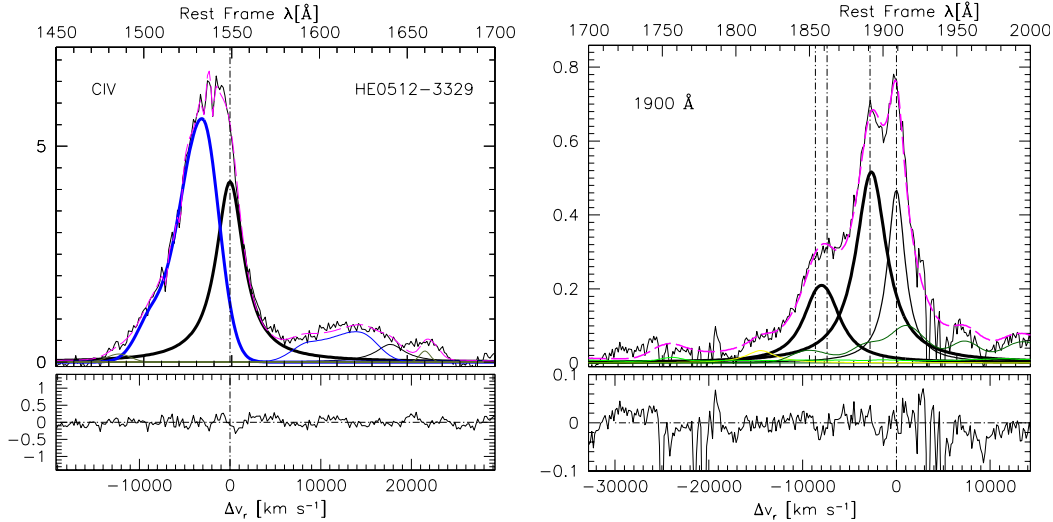


Figure 1. Left: the CIV profile of HE0512, a Population A quasar in the sample of Sulentic et al. [14]. The profile has been decomposed into a symmetric, unshifted component (the virialized component, thick black line) and a blue shifted component modeled by a skewed Gaussian (thick blue line). The flat-topped emission on the red side of CIV is mainly HeII λ 1640; **Right:** the 1900 blend for HE0512. The AlIII and SiIII lines at 1860 Å and 1892 Å are unshifted and symmetric, and their FWHMs are in agreement with the H β and of the CIV virialized component profile. The thick black components can be thought as scaled H β profiles, as in the case of CIV. Note that AlIII λ 1860 lacks the blue-shifted excess of CIV. The thin line shows the CIII λ 1909 profile whose intensity remains highly uncertain because of the heavy blending with FeIII emission.

The Vestergaard and Peterson [29] scaling laws

$$\log M_{\text{BH}} = c + a \log L + b \log \text{FWHM}, \quad (4)$$

assumed that the width of CIV and H β are equivalent, with $a \approx 0.5$, $b = 2$, and c an average constant difference between the 5100 and the 1450 luminosity. Considering the FWHM CIV as a proxy of FWHM H β causes a bias along the E1 sequence. Especially for extreme Population A, errors can be as large as 2 dex. Figure 2 is the statement of the ensuing BH mass taboo for CIV.

Figure 2 (based on the data of Sulentic et al. [6]) emphasizes a systematic trend for which a corrective could be estimated. To this aim, we defined a sample of RQ quasars with CIV λ 1549 observations including 70 sources at $z < 1$ [6], and 25 high-luminosity sources at $z > 1.4$ [14]. Matching H β data are available from our previous observations [11,82] or from published spectra. At $L > 10^{47}$ erg s $^{-1}$, high amplitude CIV 1549 blueshifts in both Population A and B are observed with median ≈ 3000 km s $^{-1}$ for Population A; two extreme cases involve CIV c(1/2) blueshift amplitude larger than 5000 km s $^{-1}$. Widespread powerful outflows are affecting both Population A and B sources [14,83] with worrisome implications for M_{BH} estimates from CIV λ 1549 FWHM.

Population A sources are more frequently selected at high z , high L . Figure 2 of [84] depicts what may be called an Eddington ratio bias: for a fixed mass, higher Eddington ratio sources are preferentially better sampled. In this way, the FWHM CIV (if left uncorrected) may lead to systematic over-estimates of M_{BH} by even one/two orders of magnitude, with the potential of creating the (spurious) result of a population of extremely massive black holes at high redshift ($z > 2$).

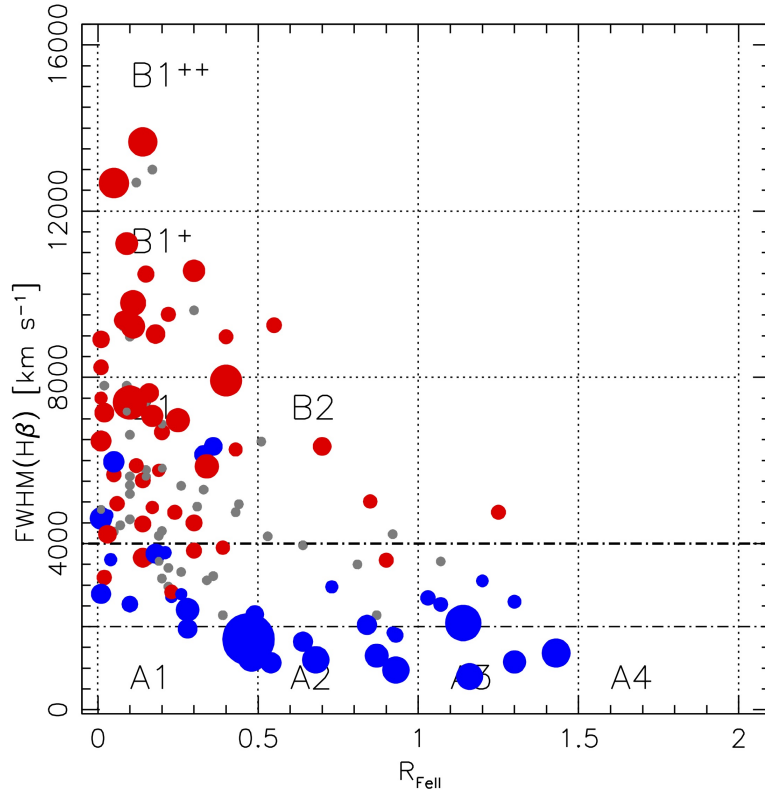


Figure 2. Bias of the M_{BH} estimates in the optical E1 plane $FWHM(H\beta)$ vs. R_{FeII} , for the full sample of Sulentic et al. [6]. Grey symbols represent differences $|\Delta \log M| = |\log M(CIV) - \log M(H\beta)| \leq 0.3$, blue dots $\Delta \log M > 0.3$, red circles $\Delta \log M < -0.3$. The size of the circles is proportional to the amplitude of the difference, with the largest blue circles showing CIV masses in excess by a factor 100. Mid-sized circles indicate a disagreement of a factor ≈ 10 . The labels identify the spectral types as described in Section 4 and the thick dot-dashed line at 4000 km s^{-1} shows the boundary between Population A and Population B.

5.4. A CIV λ 1549 VBE

The centroid shift at half-maximum $c(1/2)$ is correlated with the FWHM in the CIV line, implying that the the FWHM excess with respect to $H\beta$ is associated with a blueshifted component, as shown in Figure 1.² The comparison of Figure 1 has been possible because we have $H\beta$ observations for this source. However, $H\beta$ observations are available only for a few hundred high-redshift quasars since the line is shifted in the IR.

Nonetheless, there have been several attempts in the last few years to define scaling laws that corrected for the non/virial contamination of CIV emission. A scaling law that assumes $M_{BH} \propto FWHM^{0.5}$ [32] accounts for the over-broadening of Population A sources, but overcorrects for Population B [45]. In general, corrections dependent on L/L_{Edd} (which is correlated with FWHM of CIV, [85]) or an L/L_{Edd} proxy such as the SiIV + OIV]1400 blend/CIV 1549 ratio are promising [9] but tend not to work well for Population B. Empirical corrections based on CIV blueshift work fairly well for high- L sources only [83,86].

It is important to consider that there is a threshold in CIV shift amplitude ($c(1/2)$) at $L/L_{Edd} \approx 0.2$ [14]. There is a strong correlation with L/L_{Edd} if blueshifts are significant. There is also a weak but significant correlation with luminosity in the sample of Sulentic et al. [14]: the partial

² This happens also for MgII, but with much lower blueward displacements (few hundreds vs. few thousands km s^{-1}).

correlation coefficient between $c(1/2)$ and L (L/L_{Edd} hidden) is significant at about a 2σ confidence level. A multivariate analysis confirms the blueshift dependence on both L and L/L_{Edd} in that sample. The blueshift dependences are consistent with a radiation-driven outflow, with a slope ≈ 0.15 for $\log L$, and slope ≈ 0.5 for L/L_{Edd} . A pure dependence on L arises for L/L_{Edd} in a small range. A strong dependence on L/L_{Edd} and a weak dependence on L can be obtained under a variety of physical scenarios. We expect that strength and form of L and L/L_{Edd} correlations are sample dependent [14].

Considering the threshold and the dependence on both L and L/L_{Edd} , using $c(1/2)$ as a proxy for L/L_{Edd} , HIL CIV corrections based on $c(1/2)$ and L reduce scatter to 0.33 dex with respect to $H\beta$ estimates, providing an unbiased M_{BH} estimator. Unfortunately, the correction coefficients are different for Pops. A and B. For Population B, the correction is highly uncertain in the sample of Sulentic et al. [14], and a larger sample of sources is needed. In addition, (1) corrections derived by Coatman et al. [83] may be sample dependent because of the Eddington ratio bias; and (2) any correction based on $c(1/2)$ requires a precise estimate of the quasar rest frame of reference, which is not easily obtained from UV data. A theoretical correction requires that $c(1/2)$ CIV and ionization conditions in the BLR are accounted for, and has not been completed as yet. It is therefore not obvious whether M_{BH} estimates based on CIV can be reliable for large samples of quasars.

5.5. Intermediate Ionization Lines (IILs)

An alternative to the use of CIV is to resort to the emission lines of the 1900 Å blend, whose constituents are mainly the resonant doublet of AlIII at $\lambda 1860$ Å, and the intercombination lines SiIII] and CIII] at $\lambda 1892$ and $\lambda 1909$ Å, respectively (Table 1 of Negrete et al. [87] provides detailed information of the atomic transitions involved). We base our analysis on ≈ 80 objects of the CIV sample described in Section 5.3 for which the 1900 blend has been covered. CIII] $\lambda 1909$ measurements have serious problems: in Population A, CIII] is faint, and blended with strong and diffuse FeIII emission. In Population B, the CIII] $\lambda 1909$ line is affected by VBC. However, considering AlIII and SiIII] it is possible to obtain a VBE consistent with $H\beta$. To this aim is necessary to assume that $\text{FWHM AlIII } 1860 = \text{FWHM SiIII] } 1892$ i.e., to anchor the FWHM AlIII to FWHM SiIII] . A source of concern is that AlIII is a resonance doublet ($^2P_{3/2, 1/2}^o \rightarrow ^2S_{1/2}$) and part of its emission may originate in an outflow, where the AlIII, as does CIV, acts as a resonant scatterer of continuum photons. However, measured AlIII shifts are < 0.2 CIV shifts and the AlIII and SiIII] profiles looks fairly symmetric in the wide majority of cases (Figure 1 shows a typical case).

If we compare the FWHM of the IILs to $H\beta$, we find that it is in very good agreement with Population A. Population B IILs are narrower than $H\beta$, but a modest correction is needed to enforce an unbiased agreement: $\text{FWHM } H\beta_{\text{BC}} = 1.35 \text{ FWHM AlIII}_{\text{BC}}$. In other words, $\xi \approx 1.35$ (Table 1) is needed to rescale the line widths to the one of $H\beta$ BC assumed as a reference VBE.

6. Photoionization Masses

The ionization parameter U can be written as

$$U = \frac{Q(H)}{4\pi r_{\text{BLR}}^2 cn}, \quad (5)$$

where $Q(H)$ is the number of ionizing photons, n the hydrogen density, and c the speed of light. The expression for U can be inverted to obtain the BLR radius

$$r_{\text{BLR}} = \left(\frac{Q(H)}{4\pi U cn} \right)^{1/2}. \quad (6)$$

The radius r_{BLR} estimates from photo-ionization agree with $c\tau$ from reverberation mapping for a sample of 12 sources [76]. The photon flux $n \cdot U$ is estimated using diagnostic ratios involving AlIII 1860, SiIII] 1892, SiII 1816, CIV 1549, SiIV + OIV] 1400. The photoionization method provides an

unbiased estimator of r_{BLR} in the sample of Negrete et al. [76], but M_{BH} estimates at high L remain largely untested [88]. The photoionization method, in principle, could avoid the dispersion intrinsic to the scaling laws with L . To obtain accurate individual estimates of M_{BH} is then necessary to have an accurate knowledge of f and of orientation effects that influence the FWHM. Both are still poorly known at the time of writing.

7. Conclusions

Retrieving a VBE that is representative of the broadening due virial motions in the low-ionization part of the BLR is a major goal in order to reduce systematic and statistical effects in single-epoch M_{BH} determinations applied to large samples of quasars. The following remarks emerge from the present review.

- Low-ionization lines ($\text{H}\beta$, $\text{MgII } 2800$) provide reliable virial broadening estimators by applying corrections to the observed line width. The corrections depend on the spectral type along the E1 MS, but they are relatively small (less than 30%), and work up to the highest L of quasars.
- The HIL $\text{CIV}\lambda 1549$ is not immediately providing a reliable virial broadening estimator. The profile is broadened by an excess emission on its blue side. The shift amplitude depends on both L/L_{Edd} and L . Large shifts are observed in Population A, with Eddington ratio above a critical $L/L_{\text{Edd}} \approx 0.2$.
- It is possible to apply corrections to the observed CIV broadening, but they remain cumbersome even for Population A. Population B sources at low Eddington ratio require a different correction (still ill-defined by the analysis of Marziani et al. [45] as Population B sources are most affected by the Eddington ratio bias mentioned in Section 5.3).
- Preliminary results on the 1900 blend indicate that the IILs lines could provide a better choice than CIV; IIL FWHM measurements appear intrinsically more robust than those of CIV since they do not require corrections based on shift measurement with respect to rest frame. However, more data are needed to assess their reliability.

The ultimate solution may be to abandon scaling laws altogether and to attempt M_{BH} estimates on an individual basis, considering r_{BLR} from photoionization and $f = f(L/L_{\text{Edd}}, L, \dots)$ (where \dots indicates any relevant physical parameter, for example the spin parameter of the black hole) as well as orientation effects on the VBE along the E1 sequence.

Acknowledgments: A.d.O., and M.L.M.A. acknowledge financial support from the Spanish Ministry for Economy and Competitiveness through grant AYA2016-76682-C3-1-P. D. D. and A. N. acknowledge support from grants PAPIIT108716, UNAM, and CONACyT221398. This research is part of the projects 176003 “Gravitation and the large scale structure of the Universe” and 176001 “Astrophysical spectroscopy of extragalactic objects” supported by the Ministry of Education and Science of the Republic of Serbia.

Author Contributions: This review is partly based on the results of several research papers by the authors: [45,76] (A.N.), [12,13,45] (A.D.O.), [11,45,76,76] (D.D.), [45] (M.D.O.), [45] (M.L.M.A.), [11–13,45,76] (P.M.). For the present review, E.B., N.B., A.D.O., D.D., M.D.O. sent comments and suggestions. P.M. wrote the paper.

Conflicts of Interest: The authors declare no conflict of interest.

Abbreviations

The following abbreviations are used in this manuscript:

BC	Broad component
BLR	Broad line region
E1	Eigenvector 1
HE	Hamburg-ESO
HIL	High ionization line
IIL	Intermediate ionization line

IP	Ionization potential
ISAAC	Infrared Spectrometer and Array Camera
LIL	Low ionization line
FWHM	Full width half maximum
FWHM	Full width zero intensity
MS	Main sequence
NLSy1	Narrow-line Seyfert 1
SDSS	Sloan digital sky survey
VBE	Virial broadening estimator

References

- Berk, D.E.V.; Richards, G.T.; Bauer, A.; Strauss, M.A.; Schneider, D.P.; Heckman, T.M.; York, D.G.; Hall, P.B.; Fan, X.; Knapp, G.R.; et al. Composite Quasar Spectra from the Sloan Digital Sky Survey. *Astron. J.* **2001**, *122*, 549–564.
- Burbidge, G.R.; Burbidge, E.M. *Quasi-Stellar Objects*; Freeman: San Francisco, CA, USA, 1967.
- Marziani, P.; Sulentic, J.W. Quasar Outflows in the 4D Eigenvector 1 Context. *Astron. Rev.* **2012**, *7*, 33–57.
- Marziani, P.; Sulentic, J.W. Estimating black hole masses in quasars using broad optical and UV emission lines. *New Astron. Rev.* **2012**, *56*, 49–63.
- Shen, Y. The mass of quasars. *Bull. Astron. Soc. India* **2013**, *41*, 61–115.
- Sulentic, J.W.; Bachev, R.; Marziani, P.; Negrete, C.A.; Dultzin, D. Civ λ 1549 as an Eigenvector 1 Parameter for Active Galactic Nuclei. *Astrophys. J.* **2007**, *666*, 757–777.
- Netzer, H.; Lira, P.; Trakhtenbrot, B.; Shemmer, O.; Cury, I. Black Hole Mass and Growth Rate at High Redshift. *Astrophys. J.* **2007**, *671*, 1256–1263.
- Mejía-Restrepo, J.E.; Trakhtenbrot, B.; Lira, P.; Netzer, H.; Capellupo, D.M. Active galactic nuclei at $z \sim 1.5$: II. Black Hole Mass estimation by means of broad emission lines. *Mon. Not. R. Astron. Soc.* **2016**, *460*, 187–211.
- Brotherton, M.S.; Runnoe, J.C.; Shang, Z.; DiPompeo, M.A. Bias in C IV-based quasar black hole mass scaling relationships from reverberation mapped samples. *Mon. Not. R. Astron. Soc.* **2015**, *451*, 1290–1298.
- Brotherton, M.S.; Runnoe, J.C.; Shang, Z.; Varju, M. Further Rehabilitating CIV-based Black Hole Mass Estimates in Quasars. In Proceedings of the 228th American Astronomical Society Meeting, San Diego, CA, USA, 12–16 June 2016; Abstracts, p. 400.05.
- Marziani, P.; Sulentic, J.W.; Stirpe, G.M.; Zamfir, S.; Calvani, M. VLT/ISAAC spectra of the H β region in intermediate-redshift quasars. III. H β broad-line profile analysis and inferences about BLR structure. *Astron. Astrophys.* **2009**, *495*, 83–112.
- Marziani, P.; Sulentic, J.W.; Plauchu-Frayn, I.; del Olmo, A. Low-Ionization Outflows in High Eddington Ratio Quasars. *Astrophys. J.* **2013**, *764*, 150.
- Marziani, P.; Sulentic, J.W.; Plauchu-Frayn, I.; del Olmo, A. Is Mg II 2800 a Reliable Virial Broadening Estimator for Quasars? *Astron. Astrophys.* **2013**, *555*, A89.
- Sulentic, J.W.; del Olmo, A.; Marziani, P.; Martínez-Carballo, M.A.; D’Onofrio, M.; Dultzin, D.; Perea, J.; Martínez-Aldama, M.L.; Negrete, C.A.; Stirpe, G.M.; et al. What does Civ λ 1549 tell us about the physical driver of the Eigenvector Quasar Sequence? *arXiv* **2017**, [arXiv:1708.03187](https://arxiv.org/abs/1708.03187).
- Fabian, A.C. Observational Evidence of Active Galactic Nuclei Feedback. *Annu. Rev. Astron. Astrophys.* **2012**, *50*, 455–489.
- Kormendy, J.; Ho, L.C. Coevolution (Or Not) of Supermassive Black Holes and Host Galaxies. *Annu. Rev. Astron. Astrophys.* **2013**, *51*, 511–653.
- King, A.; Pounds, K. Powerful Outflows and Feedback from Active Galactic Nuclei. *Annu. Rev. Astron. Astrophys.* **2015**, *53*, 115–154.
- Ferland, G.J.; Hu, C.; Wang, J.; Baldwin, J.A.; Porter, R.L.; van Hoof, P.A.M.; Williams, R.J.R. Implications of Infalling Fe II-Emitting Clouds in Active Galactic Nuclei: Anisotropic Properties. *Astrophys. J. Lett.* **2009**, *707*, L82–L86.
- Marziani, P.; Carballo, M.A.M.; Sulentic, J.W.; Del Olmo, A.; Stirpe, G.M.; Dultzin, D. The most powerful quasar outflows as revealed by the Civ λ 1549 resonance line. *Astrophys. Space Sci.* **2016**, *361*, 29.
- Smith, A.; Bromm, V.; Loeb, A. The first supermassive black holes. *arXiv* **2017**, [arXiv:1703.03083](https://arxiv.org/abs/1703.03083).

21. Trakhtenbrot, B.; Urry, C.M.; Civano, F.; Rosario, D.J.; Elvis, M.; Schawinski, K.; Suh, H.; Bongiorno, A.; Simmons, B.D. An over-massive black hole in a typical star-forming galaxy, 2 billion years after the Big Bang. *Science* **2015**, *349*, 168–171.
22. Denney, K.D.; Pogge, R.W.; Assef, R.J.; Kochanek, C.S.; Peterson, B.M.; Vestergaard, M. C IV Line-width Anomalies: The Perils of Low Signal-to-noise Spectra. *Astrophys. J.* **2013**, *775*, 60.
23. Peterson, B.M.; Wandel, A. Keplerian Motion of Broad-Line Region Gas as Evidence for Supermassive Black Holes in Active Galactic Nuclei. *Astrophys. J. Lett.* **1999**, *521*, L95–L98.
24. Kaspi, S.; Smith, P.S.; Netzer, H.; Maoz, D.; Jannuzi, B.T.; Giveon, U. Reverberation Measurements for 17 Quasars and the Size-Mass-Luminosity Relations in Active Galactic Nuclei. *Astrophys. J.* **2000**, *533*, 631–649.
25. Kaspi, S.; Brandt, W.N.; Maoz, D.; Netzer, H.; Schneider, D.P.; Shemmer, O. Reverberation Mapping of High-Luminosity Quasars: First Results. *Astrophys. J.* **2007**, *659*, 997–1007.
26. Bentz, M.C.; Peterson, B.M.; Pogge, R.W.; Vestergaard, M. The Black Hole Mass-Bulge Luminosity Relationship for Active Galactic Nuclei From Reverberation Mapping and Hubble Space Telescope Imaging. *Astrophys. J. Lett.* **2009**, *694*, L166–L170.
27. Du, P.; Lu, K.X.; Hu, C.; Qiu, J.; Li, Y.R.; Huang, Y.K.; Wang, F.; Bai, J.M.; Bian, W.H.; Yuan, Y.F.; et al. Supermassive Black Holes with High Accretion Rates in Active Galactic Nuclei. VI. Velocity-resolved Reverberation Mapping of the H β Line. *Astrophys. J.* **2016**, *820*, 27.
28. Bentz, M.C.; Peterson, B.M.; Pogge, R.W.; Vestergaard, M.; Onken, C.A. The Radius-Luminosity Relationship for Active Galactic Nuclei: The Effect of Host-Galaxy Starlight on Luminosity Measurements. *Astrophys. J.* **2006**, *644*, 133–142.
29. Vestergaard, M.; Peterson, B.M. Determining Central Black Hole Masses in Distant Active Galaxies and Quasars. II. Improved Optical and UV Scaling Relationships. *Astrophys. J.* **2006**, *641*, 689–709.
30. Trakhtenbrot, B.; Netzer, H. Black hole growth to $z = 2$ – I. Improved virial methods for measuring M_{BH} and L/L_{Edd} . *Mon. Not. R. Astron. Soc.* **2012**, *427*, 3081–3102.
31. Shen, Y.; Liu, X. Comparing Single-epoch Virial Black Hole Mass Estimators for Luminous Quasars. *Astrophys. J.* **2012**, *753*, 125.
32. Park, D.; Woo, J.H.; Denney, K.D.; Shin, J. Calibrating C-IV-based Black Hole Mass Estimators. *Astrophys. J.* **2013**, *770*, 87.
33. Shen, Y.; Brandt, W.N.; Richards, G.T.; Denney, K.D.; Greene, J.E.; Grier, C.J.; Ho, L.C.; Peterson, B.M.; Petitjean, P.; Schneider, D.P.; et al. The Sloan Digital Sky Survey Reverberation Mapping Project: Velocity Shifts of Quasar Emission Lines. *Astrophys. J.* **2016**, *831*, 7.
34. Elvis, M.; Wilkes, B.J.; McDowell, J.C.; Green, R.F.; Bechtold, J.; Willner, S.P.; Oey, M.S.; Polomski, E.; Cutri, R. Atlas of quasar energy distributions. *Astrophys. J. Suppl. Ser.* **1994**, *95*, 1–68.
35. Richards, G.T.; Lacy, M.; Storrie-Lombardi, L.J.; Hall, P.B.; Gallagher, S.C.; Hines, D.C.; Fan, X.; Papovich, C.; Berk, D.E.V.; Trammell, G.B.; et al. Spectral Energy Distributions and Multiwavelength Selection of Type 1 Quasars. *Astrophys. J. Suppl. Ser.* **2006**, *166*, 470–497.
36. Runnoe, J.C.; Shang, Z.; Brotherton, M.S. The orientation dependence of quasar spectral energy distributions. *Mon. Not. R. Astron. Soc.* **2013**, *435*, 3251–3261.
37. Horne, K.; AGN STORM collaboration. Echo Mapping of the Broad Emission-Line Region in NGC 5548. *Zenodo* **2017**, doi:10.5281/zenodo.569512.
38. Pei, L.; Fausnaugh, M.M.; Barth, A.J.; Peterson, B.M.; Bentz, M.C.; De Rosa, G.; Denney, K.D.; Goad, M.R.; Kochanek, C.S.; Korista, K.T.; et al. Space Telescope and Optical Reverberation Mapping Project. V. Optical Spectroscopic Campaign and Emission-line Analysis for NGC 5548. *Astrophys. J.* **2017**, *837*, 131.
39. Fausnaugh, M.M.; Denney, K.D.; Barth, A.J.; Bentz, M.C.; Bottorff, M.C.; Carini, M.T.; Croxall, K.V.; De Rosa, G.; Goad, M.R.; Horne, K.; et al. Space Telescope and Optical Reverberation Mapping Project. III. Optical Continuum Emission and Broadband Time Delays in NGC 5548. *Astrophys. J.* **2016**, *821*, 56.
40. Bon, E.; Marziani, P.; Bon, N. Periodic optical variability of AGN. In Proceedings of the IAU Symposium 324: New Frontiers in Black Hole Astrophysics, Ljubljana, Slovenia, 12–16 September 2016; pp. 176–179.
41. Bon, E.; Jovanović, P.; Marziani, P.; Shapovalova, A.I.; Bon, N.; Borika Jovanović, V.; Borika, D.; Sulentic, J.; Popović, L.Č. The First Spectroscopically Resolved Sub-parsec Orbit of a Supermassive Binary Black Hole. *Astrophys. J.* **2012**, *759*, 118.

42. Graham, M.J.; Djorgovski, S.G.; Stern, D.; Drake, A.J.; Mahabal, A.A.; Donalek, C.; Glikman, E.; Larson, S.; Christensen, E. A systematic search for close supermassive black hole binaries in the Catalina Real-time Transient Survey. *Mon. Not. R. Astron. Soc.* **2015**, *453*, 1562–1576.
43. Bon, E.; Zucker, S.; Netzer, H.; Marziani, P.; Bon, N.; Jovanović, P.; Shapovalova, A.I.; Komossa, S.; Gaskell, C.M.; Popović, L.Č.; et al. Evidence for Periodicity in 43 year-long Monitoring of NGC 5548. *Astrophys. J. Suppl. Ser.* **2016**, *225*, 29.
44. Charisi, M.; Bartos, I.; Haiman, Z.; Price-Whelan, A.M.; Graham, M.J.; Bellm, E.C.; Laher, R.R.; Márka, S. A population of short-period variable quasars from PTF as supermassive black hole binary candidates. *Mon. Not. R. Astron. Soc.* **2016**, *463*, 2145–2171.
45. Marziani, P.; Bon, E.; Bon, N.; Dultzin, D.; Del Olmo, A.; D’Onofrio, M. **2017**, in preparation.
46. Li, Y.R.; Wang, J.M.; Ho, L.C.; Lu, K.X.; Qiu, J.; Du, P.; Hu, C.; Huang, Y.K.; Zhang, Z.X.; Wang, K.; et al. Spectroscopic Indication of a Centi-parsec Supermassive Black Hole Binary in the Galactic Center of NGC 5548. *Astrophys. J.* **2016**, *822*, 4.
47. Croom, S.M. Do quasar broad-line velocity widths add any information to virial black hole mass estimates? *arXiv* **2011**, [arXiv:1105.4391](https://arxiv.org/abs/1105.4391).
48. Woo, J.H.; Treu, T.; Barth, A.J.; Wright, S.A.; Walsh, J.L.; Bentz, M.C.; Martini, P.; Bennert, V.N.; Canalizo, G.; Filippenko, A.V.; et al. The Lick AGN Monitoring Project: The $M_{\text{BH}}-\sigma_*$ Relation for Reverberation-mapped Active Galaxies. *Astrophys. J.* **2010**, *716*, 269–280.
49. Gültekin, K.; Richstone, D.O.; Gebhardt, K.; Lauer, T.R.; Tremaine, S.; Aller, M.C.; Bender, R.; Dressler, A.; Faber, S.M.; Filippenko, A.V.; et al. The M- σ and M-L Relations in Galactic Bulges, and Determinations of Their Intrinsic Scatter. *Astrophys. J.* **2009**, *698*, 198–221.
50. Onken, C.A.; Ferrarese, L.; Merritt, D.; Peterson, B.M.; Pogge, R.W.; Vestergaard, M.; Wandel, A. Supermassive Black Holes in Active Galactic Nuclei. II. Calibration of the Black Hole Mass-Velocity Dispersion Relationship for Active Galactic Nuclei. *Astrophys. J.* **2004**, *615*, 645–651.
51. Ferrarese, L.; Merritt, D. A Fundamental Relation between Supermassive Black Holes and Their Host Galaxies. *Astrophys. J. Lett.* **2000**, *539*, L9–L12.
52. Graham, A.W.; Onken, C.A.; Athanassoula, E.; Combes, F. An expanded $M_{\text{bh}}-\sigma$ diagram, and a new calibration of active galactic nuclei masses. *Mon. Not. R. Astron. Soc.* **2011**, *412*, 2211–2228.
53. Collin, S.; Kawaguchi, T.; Peterson, B.M.; Vestergaard, M. Systematic effects in measurement of black hole masses by emission-line reverberation of active galactic nuclei: Eddington ratio and inclination. *Astron. Astrophys.* **2006**, *456*, 75–90.
54. Sulentic, J.W.; Marziani, P.; Zwitter, T.; Dultzin-Hacyan, D.; Calvani, M. The Demise of the Classical Broad-Line Region in the Luminous Quasar PG 1416-129. *Astrophys. J. Lett.* **2000**, *545*, L15–L18.
55. Sulentic, J.; Marziani, P.; Zamfir, S. The Case for Two Quasar Populations. *Open Astron.* **2011**, *20*, 427–434.
56. Fraix-Burnet, D.; Marziani, P.; D’Onofrio, M.; Dultzin, D. The Phylogeny of Quasars and the Ontogeny of Their Central Black Holes. *Front. Astron. Space Sci.* **2017**, *4*, 1.
57. Boroson, T.A.; Green, R.F. The emission-line properties of low-redshift quasi-stellar objects. *Astrophys. J. Suppl. Ser.* **1992**, *80*, 109–135.
58. Dultzin-Hacyan, D.; Sulentic, J.; Marziani, P.; Calvani, M.; Moles, M. A Correlation Analysis for Emission Lines in 52 AGN. In *IAU Colloquium 159: Emission Lines in Active Galaxies: New Methods and Techniques*; Peterson, B.M., Cheng, F.Z., Wilson, A.S., Eds.; Astronomical Society of the Pacific Conference Series; The Astronomical Society of the Pacific: San Francisco, CA, USA, 1997; Volume 113, p. 262.
59. Shang, Z.; Wills, B.J.; Robinson, E.L.; Wills, D.; Laor, A.; Xie, B.; Yuan, J. The Baldwin Effect and Black Hole Accretion: A Spectral Principal Component Analysis of a Complete Quasar Sample. *Astrophys. J.* **2003**, *586*, 52–71.
60. Kruczek, N.E.; Richards, G.T.; Gallagher, S.C.; Deo, R.P.; Hall, P.B.; Hewett, P.C.; Leighly, K.M.; Krawczyk, C.M.; Proga, D. C IV Emission and the Ultraviolet through X-Ray Spectral Energy Distribution of Radio-quiet Quasars. *Astron. J.* **2011**, *142*, 130.
61. Tang, B.; Shang, Z.; Gu, Q.; Brotherton, M.S.; Runnoe, J.C. The Optical and Ultraviolet Emission-line Properties of Bright Quasars with Detailed Spectral Energy Distributions. *Astrophys. J. Suppl. Ser.* **2012**, *201*, 38.

62. Kuraszkiewicz, J.; Wilkes, B.J.; Schmidt, G.; Smith, P.S.; Cutri, R.; Czerny, B. Principal Component Analysis of the Spectral Energy Distribution and Emission Line Properties of Red 2MASS Active Galactic Nuclei. *Astrophys. J.* **2009**, *692*, 1180–1189.
63. Mao, Y.F.; Wang, J.; Wei, J.Y. Extending the Eigenvector 1 space to the optical variability of quasars. *Res. Astron. Astrophys.* **2009**, *9*, 529–537.
64. Grupe, D. A Complete Sample of Soft X-ray-selected AGNs. II. Statistical Analysis. *Astron. J.* **2004**, *127*, 1799–1810.
65. Wang, J.; Wei, J.Y.; He, X.T. A Sample of IRAS Infrared-selected Seyfert 1.5 Galaxies: Infrared Color $\alpha(60, 25)$ -dominated Eigenvector 1. *Astrophys. J.* **2006**, *638*, 106–119.
66. Richards, G.T.; Kruczek, N.E.; Gallagher, S.C.; Hall, P.B.; Hewett, P.C.; Leighly, K.M.; Deo, R.P.; Kratzer, R.M.; Shen, Y. Unification of Luminous Type 1 Quasars through C IV Emission. *Astron. J.* **2011**, *141*, 167.
67. Yip, C.W.; Connolly, A.J.; Berk, D.E.V.; Ma, Z.; Frieman, J.A.; SubbaRao, M.; Szalay, A.S.; Richards, G.T.; Hall, P.B.; Schneider, D.P.; et al. Spectral Classification of Quasars in the Sloan Digital Sky Survey: Eigenspectra, Redshift, and Luminosity Effects. *Astron. J.* **2004**, *128*, 2603–2630.
68. Shen, Y.; Ho, L.C. The diversity of quasars unified by accretion and orientation. *Nature* **2014**, *513*, 210–213.
69. Sun, J.; Shen, Y. Dissecting the Quasar Main Sequence: Insight from Host Galaxy Properties. *Astrophys. J. Lett.* **2015**, *804*, L15.
70. Sulentic, J.W.; Marziani, P.; Zamanov, R.; Bachev, R.; Calvani, M.; Dultzin-Hacyan, D. Average Quasar Spectra in the Context of Eigenvector 1. *Astrophys. J. Lett.* **2002**, *566*, L71–L75.
71. Marziani, P.; Sulentic, J.W.; Zwitter, T.; Dultzin-Hacyan, D.; Calvani, M. Searching for the Physical Drivers of the Eigenvector 1 Correlation Space. *Astrophys. J.* **2001**, *558*, 553–560.
72. Sulentic, J.W.; Marziani, P.; Dultzin-Hacyan, D. Phenomenology of Broad Emission Lines in Active Galactic Nuclei. *Annu. Rev. Astron. Astrophys.* **2000**, *38*, 521–571.
73. Abramowicz, M.A.; Straub, O. Accretion discs. *Scholarpedia* **2014**, *9*, 2408.
74. Bon, N.; Bon, E.; Marziani, P.; Jovanović, P. Gravitational redshift of emission lines in the AGN spectra. *Astrophys. Space Sci.* **2015**, *360*, 41.
75. Wang, J.; Dong, X.; Wang, T.; Ho, L.C.; Yuan, W.; Wang, H.; Zhang, K.; Zhang, S.; Zhou, H. Estimating Black Hole Masses in Active Galactic Nuclei Using the Mg II $\lambda 2800$ Emission Line. *Astrophys. J.* **2009**, *707*, 1334–1346.
76. Negrete, C.A.; Dultzin, D.; Marziani, P.; Sulentic, J.W. Reverberation and Photoionization Estimates of the Broad-line Region Radius in Low- z Quasars. *Astrophys. J.* **2013**, *771*, 31.
77. Zamfir, S.; Sulentic, J.W.; Marziani, P.; Dultzin, D. Detailed characterization of H β emission line profile in low- z SDSS quasars. *Mon. Not. R. Astron. Soc.* **2010**, *403*, 1759–1786.
78. Leighly, K.M. ASCA (and HST) observations of NLS1s. *New Astron. Rev.* **2000**, *44*, 395–402.
79. Bachev, R.; Marziani, P.; Sulentic, J.W.; Zamanov, R.; Calvani, M.; Dultzin-Hacyan, D. Average Ultraviolet Quasar Spectra in the Context of Eigenvector 1: A Baldwin Effect Governed by the Eddington Ratio? *Astrophys. J.* **2004**, *617*, 171–183.
80. Marziani, P.; Sulentic, J.W.; Negrete, C.A.; Dultzin, D.; Zamfir, S.; Bachev, R. Broad-line region physical conditions along the quasar eigenvector 1 sequence. *Mon. Not. R. Astron. Soc.* **2010**, *409*, 1033–1048.
81. Denney, K.D.; Vestergaard, M.; Watson, D.; Davis, T. Using Quasars as Standard Candles for Studying Dark Energy. In Proceedings of the American Astronomical Society Meeting, Austin, TX, USA, 8–12 January 2012; Abstracts, Volume 219, p. 440.20.
82. Marziani, P.; Sulentic, J.W.; Zamanov, R.; Calvani, M.; Dultzin-Hacyan, D.; Bachev, R.; Zwitter, T. An Optical Spectroscopic Atlas of Low-Redshift Active Galactic Nuclei. *Astrophys. J. Suppl. Ser.* **2003**, *145*, 199–211.
83. Coatman, L.; Hewett, P.C.; Banerji, M.; Richards, G.T.; Hennawi, J.F.; Prochaska, J.X. Correcting C IV-based virial black hole masses. *Mon. Not. R. Astron. Soc.* **2017**, *465*, 2120–2142.
84. Sulentic, J.W.; Martínez-Carballo, M.A.; Marziani, P.; del Olmo, A.; Stirpe, G.M.; Zamfir, S.; Plauchu-Frayn, I. 3C 57 as an Atypical Radio-Loud Quasar: Implications for the Radio-Loud/Radio-Quiet Dichotomy. *Mon. Not. R. Astron. Soc.* **2015**, *450*, 1916–1925.
85. Saito, Y.; Imanishi, M.; Minowa, Y.; Morokuma, T.; Kawaguchi, T.; Sameshima, H.; Minezaki, T.; Oi, N.; Nagao, T.; Kawatatu, N.; et al. Near-infrared spectroscopy of quasars at $z \sim 3$ and estimates of their supermassive black hole masses. *Publ. Astron. Soc. Jpn.* **2016**, *68*, doi:10.1093/pasj/psv102.
86. Coatman, L.; Hewett, P.C.; Banerji, M.; Richards, G.T. C IV emission-line properties and systematic trends in quasar black hole mass estimates. *Mon. Not. R. Astron. Soc.* **2016**, *461*, 647–665.

87. Negrete, A.; Dultzin, D.; Marziani, P.; Sulentic, J. BLR Physical Conditions in Extreme Population A Quasars: A Method to Estimate Central Black Hole Mass at High Redshift. *Astrophys. J.* **2012**, *757*, 62.
88. Negrete, C.A.; Dultzin, D.; Marziani, P.; Sulentic, J.W. A New Method to Obtain the Broad Line Region Size of High Redshift Quasars. *Astrophys. J.* **2014**, *794*, 95.



© 2017 by the authors. Licensee MDPI, Basel, Switzerland. This article is an open access article distributed under the terms and conditions of the Creative Commons Attribution (CC BY) license (<http://creativecommons.org/licenses/by/4.0/>).